17th World Conference on Earthquake Engineering, 17WCEE
Sendai, Japan - September 13th to 18th 2020

A TWO-LEVEL FRAMEWORK FOR REGION-SPECIFIC ENGINEERING VALIDATION OF SIMULATED GROUND MOTIONS

C. Huang[1], K. Tarbali[2], C. Galasso[3], R. Paolucci[4]

[1] *Ph.D. candidate, Civil, Environmental and Geomatic Eng. Dept., University College London (UCL), UK, chen.huang.14@ucl.ac.uk*
[2] *Research Fellow, Civil, Environmental and Geomatic Eng. Dept., University College London (UCL), UK, k.tarbali@ucl.ac.uk*
[3] *Associate Professor, Civil, Environmental and Geomatic Eng. Dept., University College London (UCL), UK, and Scuola Universitaria Superiore (IUSS) Pavia, Italy, c.galasso@ucl.ac.uk*
[4] *Professor, Civil and Environmental Eng. Dept., Politecnico di Milano, Italy, roberto.paolucci@polimi.it*

Abstract

This study proposes a two-level framework for region-specific validation of simulated ground-motions, including signal-based and ground-motion model (GMM)-based statistical comparisons. The validation framework is demonstrated on the simulated broadband ground motions of the M_w 6.0 2012 May 29 Emilia-Romagna earthquake, Italy, which are generated by combing low-frequency simulated ground motions from 3D physics-based numerical simulations with high-frequency stochastic ground motions from artificial neural networks. The peak inelastic displacement (S_{di}) and the equivalent number of cycles (N_e) demands from the simulations with respect to the counterpart from recordings and empirical models are investigated. Results of the study indicate that S_{di} values of the considered single-degree-of-freedom nonlinear systems subjected to the simulated ground motions generally underestimate those from the recordings and empirical GMMs, particularly at short vibration periods. The N_e values from the simulations slightly underestimate the N_e values from the recordings and empirical GMMs. However, peculiar overestimations have been observed around the transition frequency between the low- and high-frequency simulation methods. Moreover, the GMM-based comparisons indicate that region-specific GMMs represent a better benchmark for the purpose of inelastic demand validations than GMMs established based on continental and/or global data. The proposed validation framework can assist in further securitizing the validity of simulated ground motions, providing insights regarding the possible improvements of simulation underlying components for the purpose of engineering utilization in design and seismic risk assessment exercises.

Keywords: broadband simulation, physics-based ground-motion simulation, inelastic engineering demand parameters, engineering validation

1. Introduction

Ground-motion simulations are needed in various engineering applications (e.g., seismic hazard analysis, seismic design and risk assessment of structures/infrastructure), especially for large-magnitude events at short source-to-site distances which are not well-represented in empirical ground motion datasets. Physics-based ground-motion simulation methodologies, in particular, incorporate characteristics of the rupture on the fault, propagation of seismic waves, and local near-surface soil response. Therefore, the generated ground-motion time series are expected to represent accurate estimates of earthquake-induced ground motions at sites of interest. Engineering validation of simulated ground motions is essential to investigate potential biases and inaccuracy in the underlying models utilized for the simulation, as well as to scrutinize the validity of the generated outputs to be used in the engineering practice.

Bradley et al. [1] have proposed a validation matrix for simulated ground motions considering the spatial extent and specificity of the simulations as well as the complexity of ground-motion properties and engineering demand parameters (EDPs) to be tested. The primary validation metrics (within this validation matrix) are ground-motion intensity measures (IMs) related to amplitude, frequency, and energy content, such as spectral accelerations, Fourier spectra and Arias intensity (I_A) [2]. The advanced validation metrics include the response of engineered systems and other properties of interest (e.g. polarization of ground motions) [3,4]. Inelastic engineering demands (IEDs), such as peak inelastic displacements, are among the advanced metrics that

effectively relate earthquake-induced hazard to building damage/loss. This is essential for the utilization with the confidence in simulations in performance-based design and assessment of various engineering systems.

This study proposes a two-level validation framework using IED values derived from ground motion signals (referred to as signal-based validation) and also based on ground-motion models (GMMs) in terms of the considered IEDs. The signal-based validation can be performed when recordings of historical events are available, whereas GMM-based validation is feasible for both historical and future earthquake scenarios. Specifically, in this paper, a scenario-specific simulation from the M_w 6.0 2012 May 29 Emilia-Romagna earthquake in the Po Plain, Italy [5], is chosen to demonstrate an application of the proposed framework (without adding complexities in terms of the simulation uncertainties and their spatial extents). The selected simulation method for illustrative purposes is a hybrid modelling combining (in the frequency domain) the low-frequency waveforms from 3D physics-based numerical simulations by SPEED (SPectral Elastodynamics with Discontinuous Galerkin approach) with high-frequency signals from an artificial neural network-based approach. It is worth noting that the intent here is not to provide a definitive judgement about the specific simulation method used in this study, but rather to illustrate the proposed validation metrics and approaches and discuss possible outcomes. The findings of this study, even though obtained based on limited sets of ground motion records, are in good agreement with previous similar studies. In the subsequent sections, the proposed framework is presented, and the pertinent implications are discussed.

2. Proposed validation framework

The proposed framework consists of two validation levels: signal-based comparison and GMM-based comparisons. The signal-based comparison assesses whether the IED time series (and their summary properties in terms of peak and permanent demand values) from simulations can represent those from recordings at the same sites (i.e., recording stations) for historical earthquakes. The GMM-based comparison aims at evaluating whether the IED values generated by the simulations are consistent with those predicted by empirical GMMs for past earthquakes (with no or a small number of recorded ground motions), as well as for ground motions simulated for future scenarios. It is noted that when a small number of recordings are available, the signal-based comparison may not assist in drawing statistically reliable conclusions. In such cases, empirical GMMs calibrated based on recordings from multiple historical events are considered as a benchmark to obtain the spatial distribution of validation metrics on a large geographical extent.

Two quantitative validation measures/methods are utilized for each validation level, as follows:

1. A *ratio* measure, computed as Eq. (1):

$$\text{ratio} = \log_{10}\left(\frac{\text{IED}_{\text{simulation}}}{\text{IED}_{\text{benchmark}}}\right), \tag{1}$$

   where the benchmark is the recordings in case of signal-based comparisons or the GMM estimates in case of GMM-based comparisons.

2. Statistical tests, performed to assess the significance of the differences in terms of median values and variances of the results from simulations with respect to the benchmark results. The Welch's *t*-test [6] and the two-sample *F*-test [7] are used to assess differences in the medians and variances, respectively. The Welch's *t*-test is a two-sample test based on the null hypothesis that two normal populations have equal means (without assuming equal variances and/or equal sample sizes). The two-sample *F*-test is a test based on the null hypothesis that two normal populations have the same variance. If the *p*-value of the test (i.e., the probability of observing a test statistic as extreme as, or more extreme than the observed value) is less than the chosen Type I error (e.g., 5% in this case), the evidence to reject the null hypothesis (which states the two populations are statistically different) is considered strong.

3. Engineering Systems and Inelastic Demands Considered

A set of nonlinear single-degree-of-freedom (SDoF) oscillators with varying dynamic characteristics are modeled using the OpenSees software [8]. These characteristics are:

- Elastic vibration period, T_e: 0.04s, 0.1s to 5s with 0.05s spacing;
- Strength reduction factor, R: 2, 4, 6, 8 and 10;
- Hysteretic models: a bilinear model with 3% post-elastic stiffness ratio (α_s);
- Equivalent viscous damping ratio, ζ: 5%.

The considered IEDs are:

- Peak inelastic displacement (S_{di}), defined as the maximum inelastic displacement;
- Equivalent number of cycles (N_e), defined as the cumulative hysteretic energy, evaluated as the sum of the areas of the hysteretic cycles (not considering the contribution of viscous damping) normalized with respect to the largest cycle, evaluated as the area underneath the monotonic backbone curve from the yielding displacement to the peak inelastic displacement [9].

The constant-R approach is adopted in this study to ensure that nonlinearity is reached for all oscillators. Thus, the yield strength (F_y) varies from recording to recording, see [9] for a discussion on this aspect. For the nonlinear dynamics analysis (NLDA), only the horizontal North-South (NS) and East-West (EW) components of ground motions are used. The geometric means of IEDs are combined from the analyses of the two components. Note that in [5] the comparison between records and simulations shows better results in the NS ground-motion component rather than the EW one. However, the use of geometric means enables a comparison with existing GMMs for the considered IEDs.

4. Case-study application

The results from physics-based ground motion simulation of the M_w 6.0 2012 May 29 Emilia-Romagna earthquake, Italy [5] are chosen as case-study simulations to demonstrate the proposed framework. Fig. 1 shows the basin depth and the location of recording stations within the simulation domain. The low-frequency ground motions are generated based on the spectral element method using the SPEED package [10]. The resulting simulations are then combined with high-frequency ground motions by correlating the high-frequency content to the simulated low-frequency ground motions. This is done by using the artificial neural networks (ANN) approach of Paolucci et al [11]. The broadband ground motions utilized in this study are obtained by merging the high- and low-frequency contents at 1.5Hz.

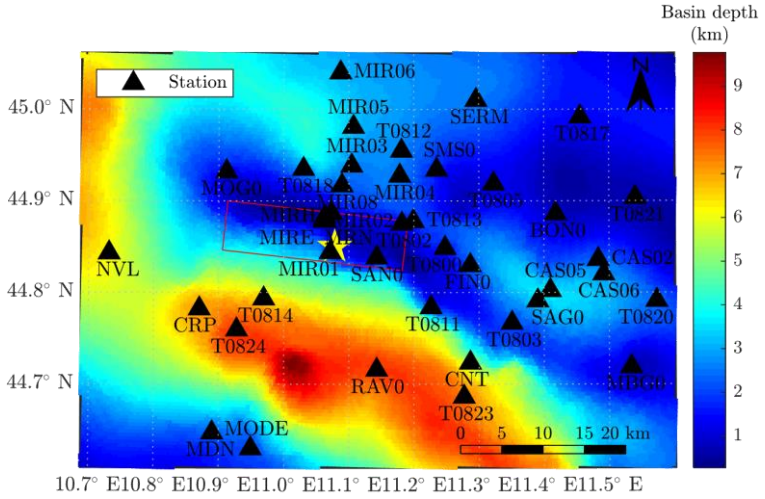

Fig. 1 – Basin depth and the location of recording stations within the simulation domain.

It is noted that the low-frequency simulated ground motions (up to about 1.5Hz) have been previously validated in terms of elastic engineering demands against recordings and empirical GMMs [5], and a generally

good agreement has been found between simulations and recordings in both time and frequency domains, especially for the horizontal NS and the vertical component. The ANN-based methodology to estimate the high-frequency content has also been validated previously [11]. Building on top of these primary validations, the proposed framework is applied to the aforementioned inelastic demand parameters.

5. Results and discussion

5.1 Signal-based ratio

There are 41 stations within the simulated domain, as shown in Fig. 1. The processed recordings from these stations are collected from the ITalian ACcelerometric Archive (ITACA) (http://itaca.mi.ingv.it/; last accessed Dec 2019) and the considered SDoF systems were subjected to the corresponding recorded and simulated ground motions. The signal-based ratios in terms of S_{di} for several representative T_e-R pairs are shown in Fig. 2, together with the 16th, 50th, and 84th percentiles of the ratios for four distance bins (i.e., R_{JB} = 0, 5±5 km, 15±5 km, 25±5 km). It is noted that the R_{JB} distance metric, i.e., the closest distance to the surface projection of ruptured fault plane, is chosen in this study in order to be able to make comparisons with the available GMM for S_{di} and N_e (elaborated on in Section 5.4) which are using R_{JB} as their distance metrics.

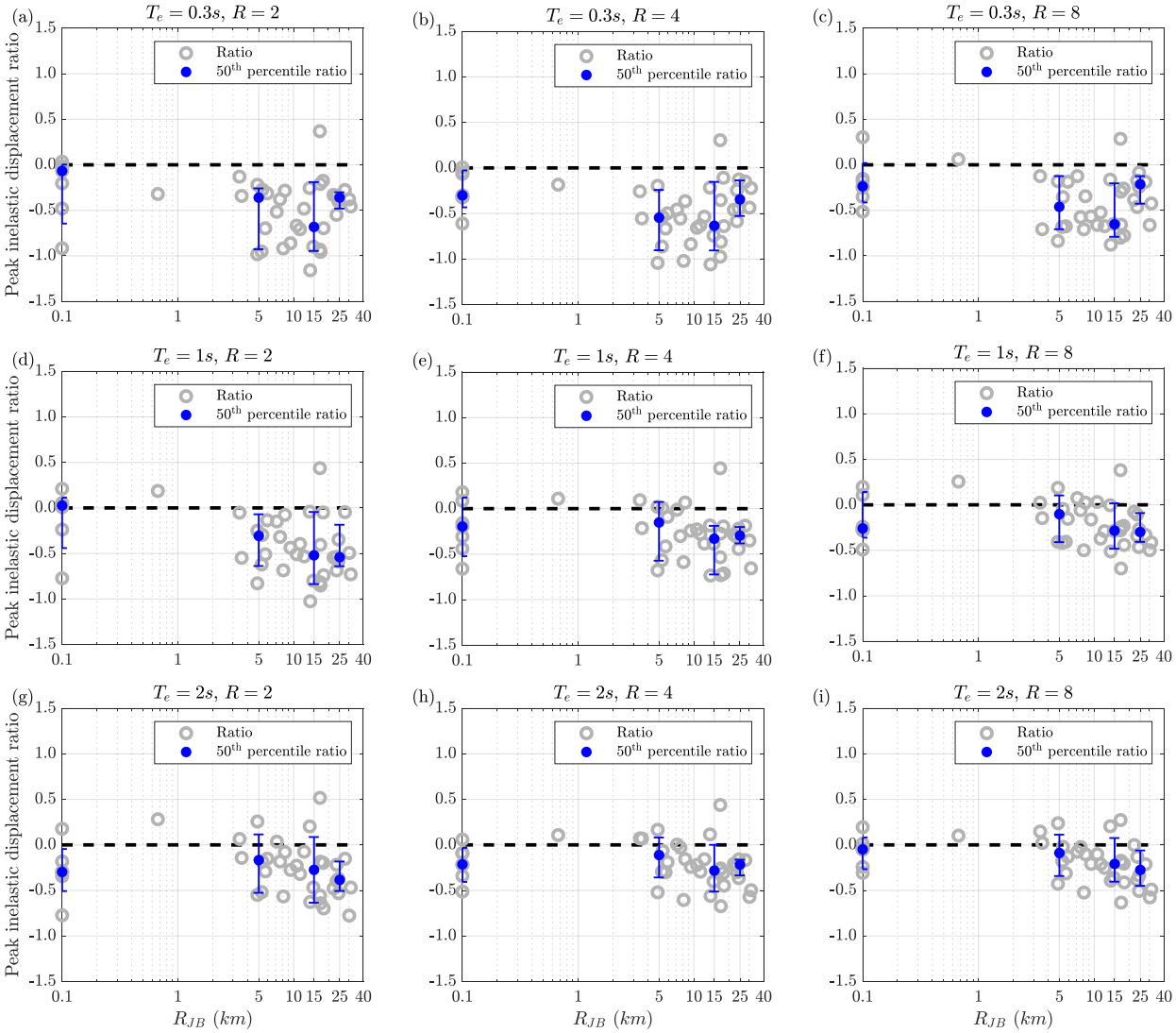

Fig. 2 – Signal-based ratios in terms of S_{di} versus R_{JB} distance for elastic periods T_e = 0.3s, 1s and 2s and reduction factor R = 2, 4 and 8. The whiskers indicate the 16th to 84th percentiles.

Negative values for the considered ratio indicate that the simulations underestimate IED values from the recordings while positive values indicate overestimations. As shown in Fig. 2, the simulations generally underestimate the S_{di} values from the recordings. The average ratio slightly decreases as the source-to-site distance increases for all T_e-R pairs. For a given distance bin and T_e, the average ratio and the associated variability slightly decrease as the strength reduction factor R increases, particularly at long periods ($T_e \geq$ 1s). Furthermore, the variabilities for bins with $R_{JB} \leq$ 15 km are larger than those with R_{JB} > 15 km for any T_e-R pair.

It is worth noting that these results are consistent with those in [5] for elastic spectral ordinates. In particular, a good agreement between records and simulations is generally observed close to the source, especially because the data collected was suitable only to constrain the velocity model in the near-fault region. Therefore, the negative bias of simulations with respect to records, especially at large distances, does not reflect an intrinsic limitation of the numerical simulation methodology.

The signal-based ratios in terms of N_e for representative T_e-R pairs are shown in Fig. 3. It is shown that the N_e values computed from simulations are generally similar to those from the recordings, except at T_e = 1s at which simulations overestimate the results from recordings for large R values. The discrepancy at periods close to the transition period of 0.75s (1.5 Hz) can be attributed to the physically incompatible level of energy from the merged low- and high-frequency simulated ground motions. The discrepancy around T_e = 1s indicates that the hybrid method can be improved. Fig. 3 also shows that the N_e variability for distance bins increases as R increases for a given T_e.

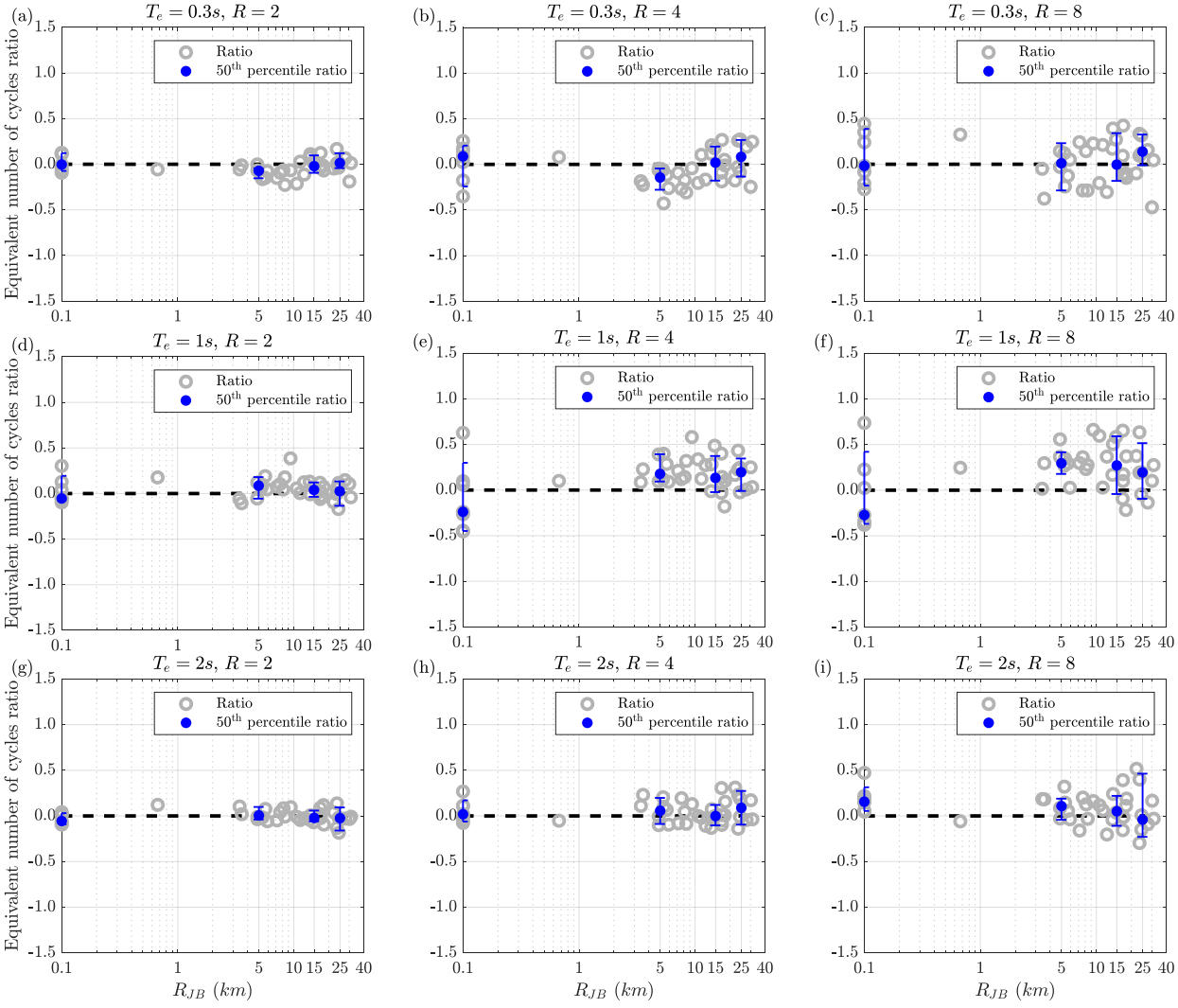

Fig. 3 – Signal-based ratios in terms of N_e versus R_{JB} distance for elastic periods T_e = 0.3s, 1s and 2s and reduction factor R = 2, 4 and 8. The whiskers indicate the 16th to 84th percentiles.

5.2 Signal-based statistical tests

The *p*-values of the statistical tests in terms of S_{di} for each T_e-R pair are summarized in Fig. 4, assuming that the peak and cyclic engineering demand parameters follow a lognormal distribution (e.g., [9], [12]). The results of the statistical tests show that the differences in the median values between the simulated and recorded ground motions are statistically significant at short periods across all R values and at moderate periods for low R values. The difference in variances is not statistically significant for any T_e-R pair.

In particular, the small values of p are clustered at short and moderate periods across different R values. This may be because the ground-motion properties in the short and moderate period range are influenced by the adopted high-frequency simulation approach. It is recalled that the high-frequency content is generated using the stochastic approach of Sabetta and Pugliese [13] which is then scaled to represent the target response spectrum from the ANN model [11]. The high- and low-frequency ground motions are then combined at the transition frequency to generate the hybrid broadband motion. In particular, given the challenges in constraining the velocity model (as discussed above) in the far-fault region, the discrepancies found in terms of long-period simulations affect the high-frequency simulations obtained through the ANN approach.

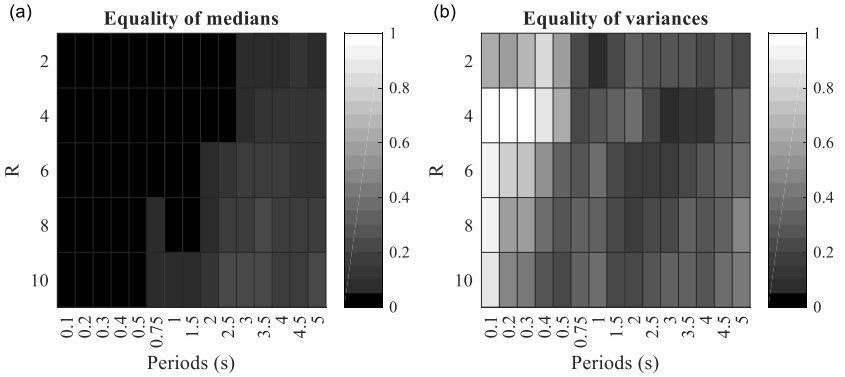

Fig. 4 – Statistical test *p*-value for S_{di}; (a) equality of medians (b) equality of variances

The results of the statistical tests on the medians and variances of N_e are summarized in Fig. 5. It is shown that the difference in the median values between the simulated and recorded ground motions is statistically significant at moderate periods for high R values. Regarding the variances, the results from the simulations are significantly different from those from the recordings at certain short and moderate periods across R. The discrepancies in medians and variances may be due to the difference in the energy content between the simulated high-frequency ground motions and the recordings (as discussed further in the next subsection).

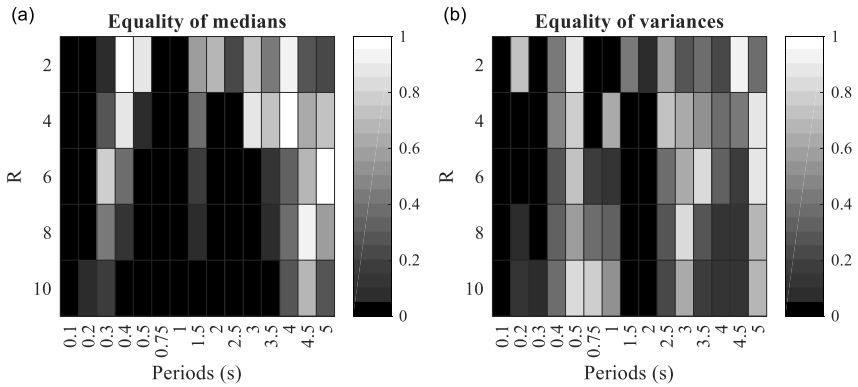

Fig. 5 – Statistical test *p*-value for N_e; (a) equality of medians (b) equality of variances.

5.3 Comparisons based on integral IMs

To further evaluate potential causes of the differences between IED values from simulations and those from recordings, the log-log scatter plots of S_{di} against integral IMs, i.e., 5%-75% significant duration ($D_{s5\text{-}75}$) and Arias Intensity (I_A), are presented in Fig. 6. It is shown that the correlation between S_{di} and $D_{s5\text{-}75}$ and between S_{di} and I_A are similar for both simulations and recordings. However, the $D_{s5\text{-}75}$ values for the simulations are clustered in a smaller range compared to those from recordings (i.e., simulation are not representing well the recordings in terms of variability in the energy content). At a given S_{di} value, the I_A values for simulations are smaller than those from recordings. These results suggest that the simulated ground motions have smaller total energy content and short significant duration compared to recordings.

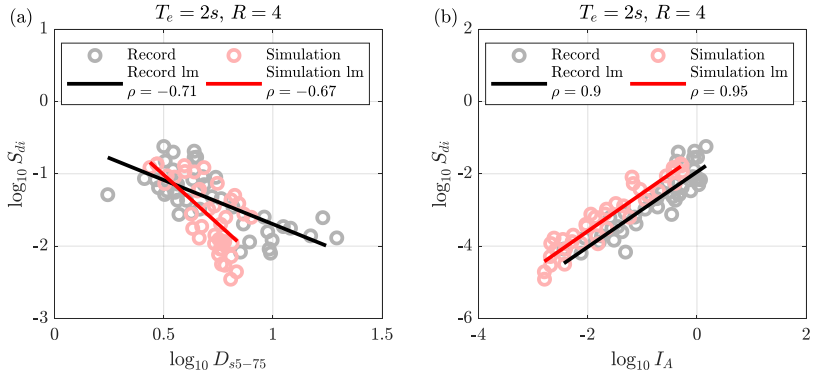

Fig. 6 – Scatter plots of $\log_{10} S_{di}$ for T_e = 2s against (a) $\log_{10} D_{s5\text{-}75}$ and (b) $\log_{10} I_A$. lm stands for linear model.

The log-log scatter plots of N_e against $D_{s5\text{-}75}$ and I_A are presented in Fig. 7. It is shown that the correlation between the N_e and $D_{s5\text{-}75}$ of simulations is not apparent compared to those from recordings. Moreover, the $D_{s5\text{-}75}$ values of simulations cover a smaller range than those of recordings. The correlation between N_e and I_A of simulations is slightly higher than those from recordings, and for a given N_e value, the I_A values of simulations are smaller than those from recordings.

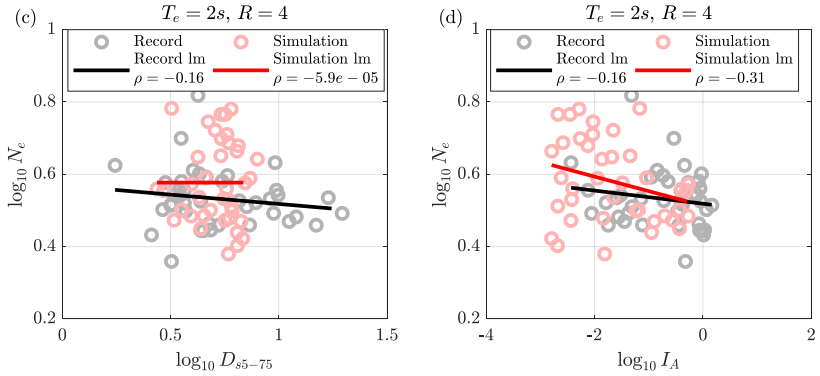

Fig. 7 – Scatter plots of $\log_{10} N_e$ for T_e = 2s against (a) $\log_{10} D_{s5\text{-}75}$ and (b) $\log_{10} I_A$. lm stands for linear model.

5.4 GMM-based ratio

The GMMs used for comparison in this study are [14], [15] for the geometric mean of S_{di} and N_e based on the ITACA database and Akkar and Sandıkkaya (2019) [16] for S_{di} and S_{di}/S_{de} based on the Pan-European RESORCE database (hereafter D11 and AS19), as shown in Table 1. According to ITACA, the sites considered in this study belong to Eurocode 8 soil class C and the corresponding V_{S30} values (time-averaged shear-wave velocity in the upper 30m of the soil profile) are obtained either from site-specific measurements provided by ITACA or estimated from geological, topographical and geophysical data [17].

The GMM-based ratios in terms of S_{di} for representative T_e-R pairs are presented in Fig. 8. It is shown that the simulation underestimates the response predicted by both GMMs, particularly at larger distances. However,

the ratios with respect to D11 are close to zeros than those of AS19. Moreover, the 50th percentile of the ratios generally decreases as the source-to-site distance increases for all T_e-R pairs. The absolute value of the 50th percentiles generally reduces as the elastic period T_e increases. Furthermore, the demand ratio variability for both models generally decreases with distance, and are slightly smaller for D11 than that for AS19.

Table 1 – GMMs considered for inelastic engineering demands

GMM	IEDs	α_s(%)	R	T_e (s)	Dataset	# Records	M_w	Distance(km)	Soil
D11[18]	S_{di}, N_e	5	2-8	0.04-2	ITACA	747	4.1-6.9	R_{JB}≤200	EC8 site class
AS19[16]	S_{di}, S_{di}/S_{de}	3	1.5-6	0.05-4	RESORCE	1041	4-7.6	R_{JB} ≤200	V_{s30}

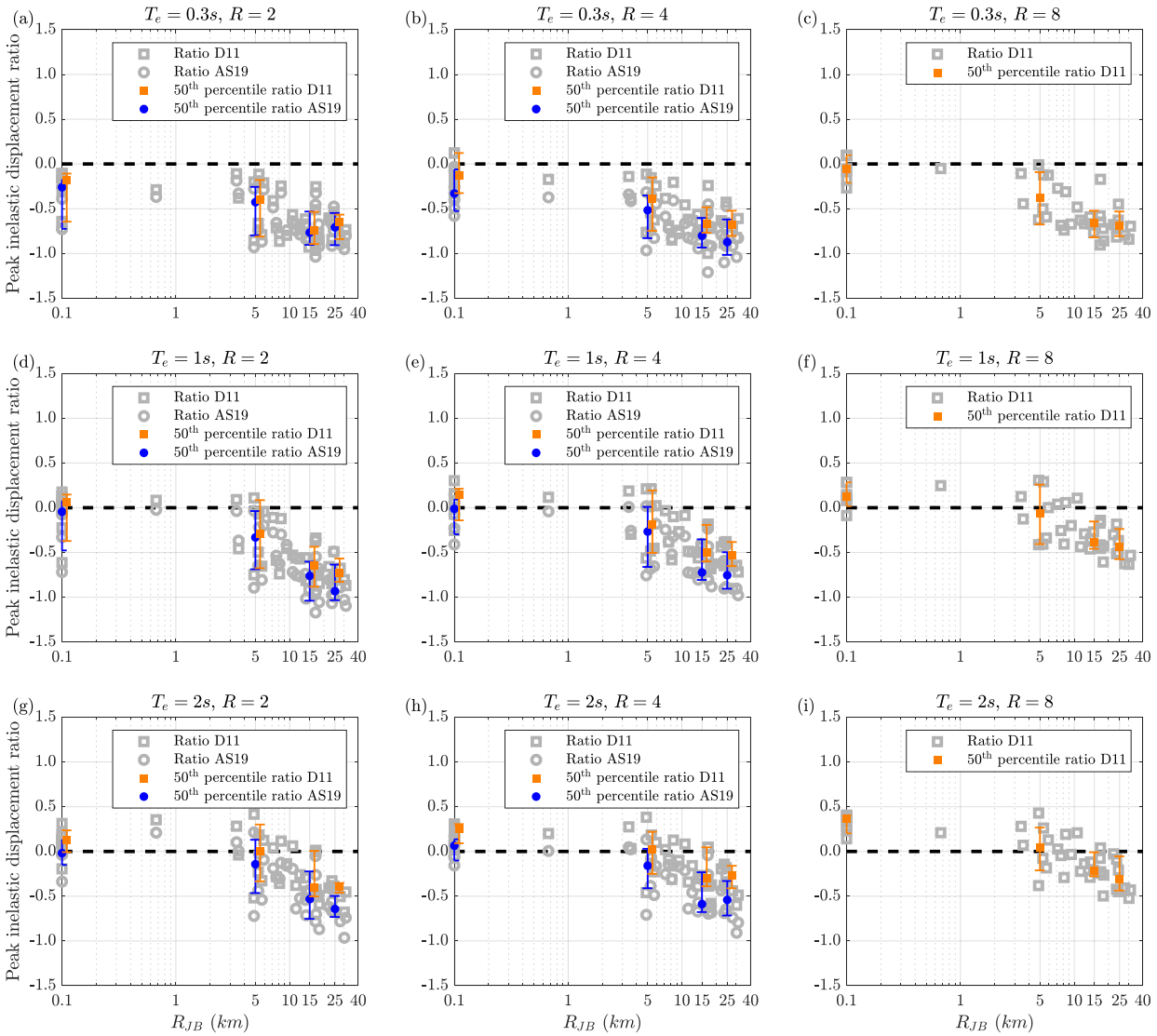

Fig. 8 – S_{di} GMM-based ratio versus R_{JB} distance for elastic periods T_e = 0.3s, 1s and 2s and reduction factor R = 2, 4 and 8. The whiskers indicate the 16th to 84th percentiles.

The differences in the GMM-based ratios (and their variabilities) between D11 and AS19 models may be due to the fact that the D11 model is developed considering Italian ground-motion data only, offering a better benchmark for the considered case study, while AS19 is developed based on a larger European dataset.

This implies that region-specific GMMs could represent more appropriate benchmarks to validate region-specific simulation results.

The GMM-based ratios in terms of N_e are presented in Fig. 9. It is shown that the simulations slightly underestimate the N_e values from the recordings, with the exception of responses around T_e = 1s. The variabilities for each distance bin increase as R increases for a given T_e. As mentioned before, the peculiar observations around T_e = 1s may be due to the inconsistency between the energy content of the merged low- and high-frequency simulated ground motions with respect to the recordings.

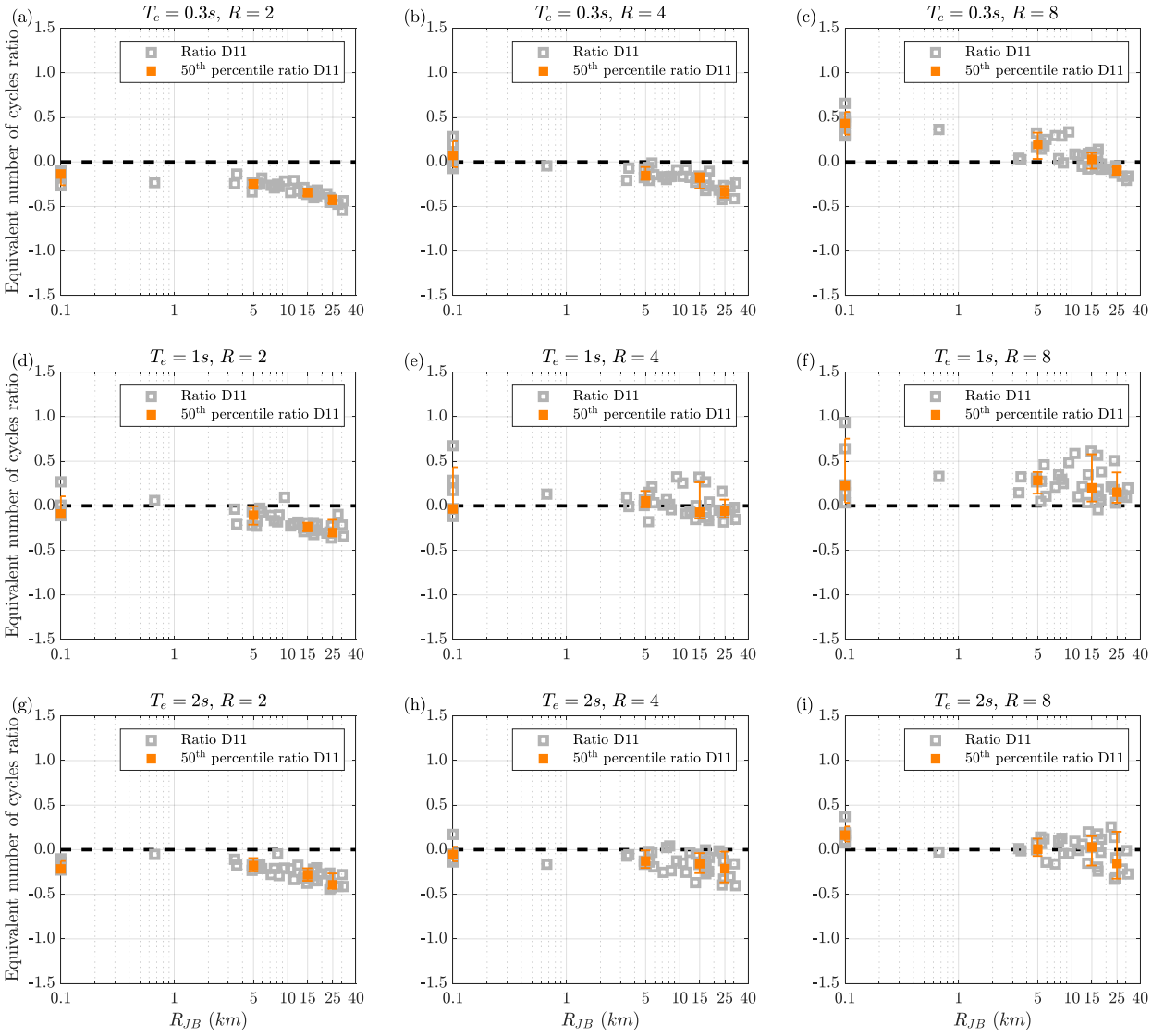

Fig. 9 – N_e GMM-based ratio versus R_{JB} distance for elastic periods T_e = 0.3s, 1s and 2s and reduction factor R = 2, 4 and 8. The whiskers indicate the 16th to 84th percentiles.

5.5 Comparison between the signal- and GMM-based ratios

The median of signal- and GMM-based ratios in terms of S_{di} and N_e are presented in Fig. 10. It is shown that the simulations generally underestimate the values from both the recordings and GMMs. Also, for the long period oscillators with high reduction factors, the GMM-based ratios of S_{di} and N_e are similar to the signal-based ratios. The N_e ratios show peaks around T_e = 1s (close to the transition frequency between the low- and high-frequency simulations) with respect to both recordings and GMMs. The ratios in terms of S_{di} for D11 are slightly smaller (in the absolute value) than those of AS19, indicating that region-specific GMMs may have

higher predictive capabilities than the generic GMMs which can be utilized in the validation of simulated ground motions for region-specific prospective scenarios.

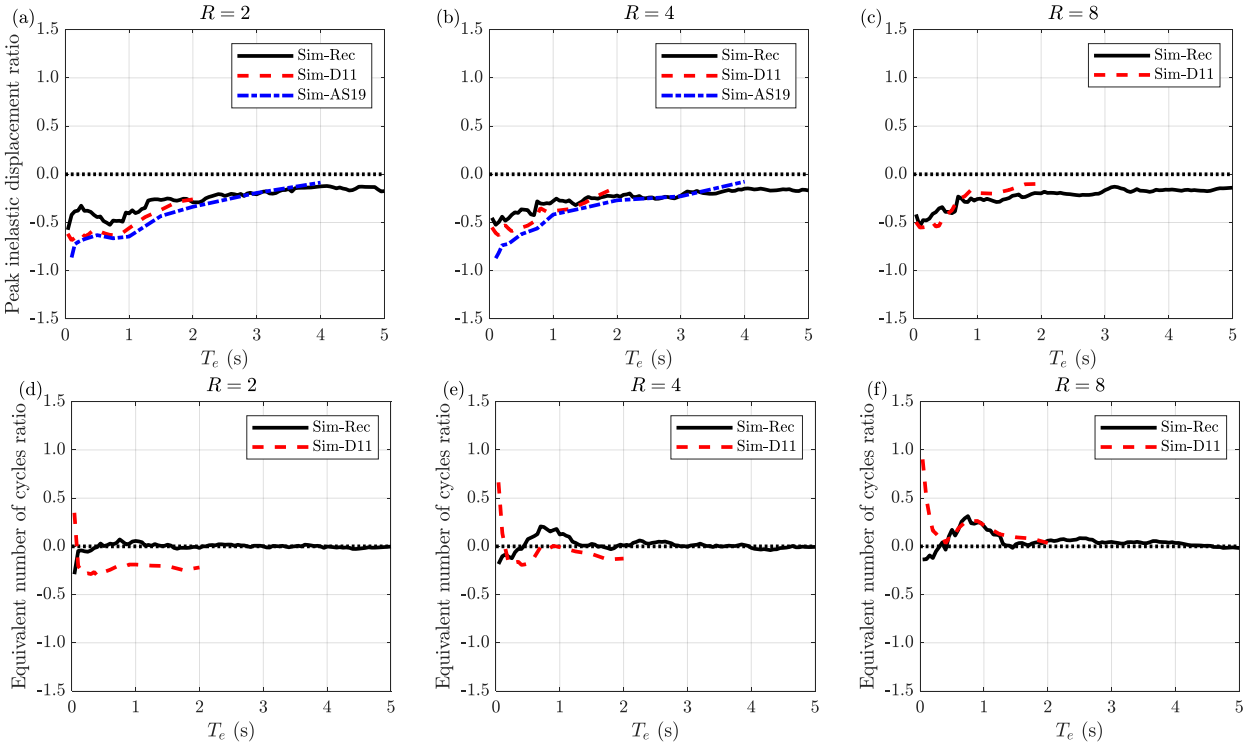

Fig. 10 Median signal- and GMM-based ratio versus periods T_e (s) for S_{di} (upper) and N_e (lower)

5.6 Future work

The differences between the simulated and benchmark results can be scrutinized spatially. At the signal level, it is expected that there will be enough observations for spatial analysis (e.g., repeated observations of ground motions at every pair of sites of interest to depict the stationary or nonstationary properties in ground motion characteristics). However, this is often not the case. At the GMM level, this requires models that are capable of representing region-specific ground motions (and their spatial correlation and cross-correlations), as well as region-specific IEDs. The spatial comparison of the results is particularly helpful in identifying physical peculiarities in the source, path, and site components that contribute to the differences between the simulation and benchmark results. The results of such comparisons may provide insights for revisiting the adopted assumptions and/or methodologies for ground motion simulation, as discussed above. Future work will address the GMM-based validation of inelastic engineering demand parameters by developing region-specific models.

6. Conclusions

This study has proposed a two-level framework for region-specific validation of simulated ground motions. The first level is the signal-based comparisons using available ground motion recordings and the second level is the GMM-based comparison using empirical GMMs as the benchmark for validation. The proposed framework can assist in providing insights regarding the possible improvements to the underlying models and approaches utilized in the simulation process. The validation framework has been demonstrated based on the peak inelastic displacement (S_{di}) and the equivalent number of cycles (N_e) demand parameters of a simulation from the M_w 6.0 2012 May 29 Emilia-Romagna earthquake, Italy. The results indicate that the considered SDoF systems with short periods subjected to the simulated ground motions have lower S_{di} when compared with the corresponding recordings. The N_e from simulations are slightly lower than those from the recordings; however, peculiar overestimations have been observed around the broadband transition period, which can be

attributed to the physically incompatible level of energy from the merged low- and high-frequency simulated ground motions. Moreover, the simulated ground motions have smaller energy content and short significant duration when compared to the corresponding recordings. All these discrepancies, particularly observed in the far-fault region, were partly expected because of the scarcity of data to constrain the velocity model in that region. Therefore, any observed bias, especially as distance increases, does not reflect an intrinsic limitation of the numerical simulation method used in this study. Furthermore, the GMM-based comparisons indicated that region-specific GMMs may have higher predictive capabilities than the generic GMMs which can be utilized in the validation of simulated ground motions for region-specific prospective scenarios. Future work will address the GMM-based validation of inelastic engineering demand parameters by developing region-specific models.

7. References

[1] Bradley BA, Pettinga D, Baker JW, Fraser J (2017): Guidance on the utilization of earthquake-induced ground motion simulations in engineering practice. *Earthquake Spectra*, **33**(3), 809–835.

[2] Anderson JG (2004): Quantitative measure of the goodness-of-fit of synthetic seismograms. *13th World Conference of Earthquake Engineering 13WCEE*, Vancouver, British Columbia, Canada.

[3] Olsen KB, Mayhew JE (2010): Goodness-of-fit criteria for broadband synthetic seismograms, with application to the 2008 M_w 5.4 Chino Hills, California, Earthquake. *Seismological Research Letter*, **81**(5),715–723.

[4] Burks LS, Baker JW (2014): Validation of ground-motion simulations through simple proxies for the response of engineered systems. *Bulletin of the Seismological Society of America*, **104**(4), 1930–1946.

[5] Paolucci R, Mazzieri I, Smerzini C (2015): Anatomy of strong ground motion: Near-source records and three-dimensional physics-based numerical simulations of the M_w 6.0 2012 May 29 Po plain earthquake, Italy. *Geophysical Journal International*, **203**(3), 2001–2020.

[6] Welch BL (1938): The significance of the difference between two means when the population variances are unequal. *Biometrika*, **29**, 350–362.

[7] Mood MA, Graybill FA, Boes DC (1974): *Introduction to the Theory of Statistics*. New York: McGraw-Hill.

[8] OpenSees. https://opensees.berkeley.edu

[9] Mazzieri I, Stupazzini M, Guidotti R, Smerzini C (2013): SPEED: SPectral Elements in Elastodynamics with Discontinuous Galerkin: a non-conforming approach for 3D multi-scale problems. *International Journal for Numerical Methods in Engineering*, **95**, 991–1010.

[10] Paolucci R, Gatti F, Infantino M, Smerzini C, Güney Özcebe A, Stupazzini M (2018): Broadband ground motions from 3D physics‐based numerical simulations using artificial neural networks. *Bulletin of the Seismological Society of America*, **108**(3A), 1272‐1286.

[11] Galasso C, Zareian F, Iervolino I, Graves RW (2012): Validation of ground-motion simulations for historical events using SDoF systems. *Bulletin of the Seismological Society of America*, **102**(6), 2727–2740.

[12] Stafford PJ, Sullivan TJ, Pennucci D (2016): Empirical correlation between inelastic and elastic spectral displacement demands. *Earthquake Spectra*, **32**(3), 1419–1448.

[13] Sabetta F, Pugliese A (1996): Estimation of response spectra and simulation of nonstationary earthquake ground motions. *Bulletin of the Seismological Society of America*, **86**(2), 337–352.

[14] De Luca F (2011): *Record, Capacity Curve Fits and Reinforced Concrete Damage States Within a Performance Based Earthquake Engineering Framework*. Ph.D. thesis, University of Naples Federico II.

[15] Akkar S, Sandıkkaya MA (2019): A ground motion model to estimate nonlinear deformation demands from a recent Pan‐European strong motion database strong-motion database. *Society for Earthquake and Civil Engineering Dynamics 2019 conference SECED2019*, Greenwich, London, U.K.

[16] Forte G, Chioccarelli E, De Falco M, Cito P, Santo A, Iervolino I (2019): Seismic soil classification of Italy based on surface geology and shear-wave velocity measurements. *Soil Dynamics and Earthquake Engineering*, **122**, pp. 79–93.

